# Atomic-Scale Structure of Nanosized Titania and Titanate: Particles, Wires, and Tubes

Swapan K. Pradhan,[†,‡] Yuanbing Mao,[§] Stanislaus S. Wong,[§,||] Peter Chupas,[⊥] and Valeri Petkov*,[†]

*Department of Physics, Central Michigan University, 203 Dow Science, Mount Pleasant, Michigan 48859, Department of Chemistry, State University of New York at Stony Brook, Stony Brook, New York 11794-3400, Condensed Matter Physics and Materials Sciences Department, Brookhaven National Laboratory, Building 480, Upton, New York 11973, and Advanced Photon Source, Argonne National Laboratory, Argonne, Illinois 60439*

*Received July 18, 2007. Revised Manuscript Received September 22, 2007. Accepted September 25, 2007*

The atomic-scale structure of nanosized "$TiO_2$-type" materials of different morphologies, including particles, wires. and tubes, has been determined by total X-ray diffraction and atomic pair distribution function analysis. Atoms in dense-filled materials such as nanoparticles and nanowires are found to form a three-dimensional network of $TiO_6$ octahedra, similar to that occurring in bulk $TiO_2$. Atoms in hollow materials such as nanotubes are arranged in corrugated layers of $TiO_6$ octahedra. The study calls attention to the often overlooked fact that a material's morphology and atomic ordering may be strongly correlated at the nanoscale.

## Introduction

The exploding field of nanoscience and technology includes the design, characterization, production, and application of structures and devices by controlling the shape and size at the nanometer scale. At such a miniature scale, many ordinary rules of physics and chemistry no longer apply and properties of nanosized and bulk materials can differ substantially. For example, both bulk graphite and carbon nanotubes are made from graphene sheets but graphite is soft, whereas carbon nanotubes are 100 times stronger than steel. The different properties arise from the different ways in which atoms in these two materials arrange in space: in thick flat stacks and slim scrolls of graphene sheets, respectively. Obviously, future progress in the field depends critically on the ability to determine the three-dimensional (3D) atomic arrangement in nanosized materials. Bulk crystalline materials usually come in well-defined shapes and morphologies, reflecting the periodic ordering of atoms inside them. However, nanosized materials increasingly are tailored into shapes that do not occur naturally with bulk materials. Hence, the shape/morphology and the atomic structure of nanosized materials may not necessarily reflect each other in an obvious way. That is why they are to be studied carefully and independently.

The morphology of materials, including nanosized ones, may be revealed by a number of techniques such as small-angle X-ray scattering and atomic force, optical, and/or electron microscopy that are already well established and widely used. Traditionally, the 3D structure of bulk materials is determined by an analysis of the peaks in their X-ray diffraction (XRD) patterns and described in terms of a small number of parameters such as lattice symmetry, lattice unit cell, and constituent atoms. Acquiring precise knowledge about the 3D structure of nanosized materials, however, is still a challenging task.[1] The reason is that atoms in nanosized materials are ordered over distances of a few nanometers only and thus act as a diffraction grating of a substantially limited length when irradiated with X-rays. As a result, the XRD patterns of nanosized materials show both Bragg-like peaks and a diffuse component. The peaks are, however, not as sharp or as plentiful as those in the XRD patterns of the corresponding bulk solids. Also, the diffuse component is very strong and cannot be neglected. This renders the traditional (i.e., Bragg) XRD analysis very difficult, if not impossible, to apply. Recently, it was shown that an approach based on the total XRD and atomic pair distribution function (PDF) data analysis can yield the 3D structure of nanosized materials in detail.[2–5] Herein, we apply the approach to nanosized titania and titanate materials of very different morphologies, including particles, wires, and tubes. The purpose of the study is 2-fold: first, to provide new structural information for these technologically important materials used in applications such as environmental purification, photocatalysis, gas sensing, and solar cells,[6–9] and, second,

* Corresponding author. E-mail: petkov@phy.cmich.edu.
† Central Michigan University.
‡ On leave from Department of Physics, The University of Burdwan, Golapbag, Burdwan 713104, West Bengal, India.
§ State University of New York at Stony Brook.
|| Brookhaven National Laboratory.
⊥ Argonne National Laboratory.

(1) Billinge, S. J. L.; Levin, I. *Science* **2007**, *316*, 561.
(2) Egami, T.; Billinge, S. J. L. In *Underneath the Bragg peaks*; Pergamon Press: New York, 2003.
(3) Petkov, V.; Zavalij, P. Y.; Lutta, S.; Whittingham, M. S.; Parvanov, V.; Shastri, S. *Phys. Rev. B* **2004**, *69*, 085410.
(4) Petkov, V.; Gateshki, M.; Niederberger, M.; Ren, Y. *Chem. Mater.* **2006**, *18*, 814.
(5) Petkov, V.; Ohta, T.; Hou, Y.; Ren, Y. *J. Phys. Chem. C* **2007**, *111*, 714.
(6) Tans, S. J.; Verschueren, A. R. M.; Dekker, C. *Nature* **1998**, *49*, 393.

10.1021/cm7019069 CCC: $37.00 
Published on Web 11/07/2007

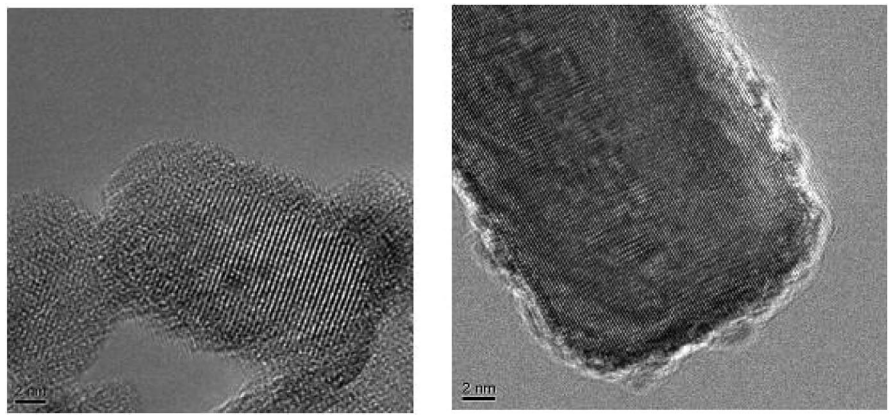


**Figure 1.** TEM images of a titania (sodium-free) NP (left) and NW (right). Both are dense-filled materials of very good crystallinity.

to investigate the relationship between the morphology and atomic-scale structure of nanosized materials, oxides in our case. Here, we are motivated by the emerging evidence that a nanosized material of complex morphology may not possess exactly the atomic structure and composition of its bulk counterpart.[3] We do find that the atomic ordering in dense-filled nanosized materials such as titania nanoparticles (NPs) and nanowires (NWs) is similar to that of bulk anatase. Hollow nanosized materials such as nanotubes (NTs), however, are built of corrugated layers of Ti-$O_6$ octahedra that do not occur in any of the three stable modifications of bulk $TiO_2$. Our findings provide additional strong evidence that the morphology and atomic-scale structure of materials may be strongly correlated at the nanoscale. We hope this will stimulate more studies along this line.

## Experimental Section

**Materials Preparation.** Several methods for the preparation of "$TiO_2$-type" materials of very fine size have been previously reported. It has been shown that, by using suitable chemicals and by tuning the synthesis process, nanosize particles with the structure of any of the known titania polymorphs—anatase, brookite, or rutile—can be obtained in a controllable way.[10] Efficient methods for the synthesis of "$TiO_2$-type" NWs and NTs have been reported as well.[11–19]

We employed a hydrothermal method[19,20] involving a reaction between bulk $TiO_2$ powder and a concentrated NaOH solution. Initially, 0.1–1 g of a commercial anatase $TiO_2$ powder was dispersed in 18 mL of an aqueous NaOH (5–10 N) solution and placed into a Teflon-lined autoclave, which was subsequently heated in an oven at 110–190 °C for 12 h to 1 week in duration. The white precipitate obtained upon filtration of the solution was purified by washing repeatedly with distilled and deionized water (100–200 mL) until the pH value of the filtrate approached 7. The as-produced sodium-based NTs or NWs (depending on the hydrothermal processing temperatures) were isolated after centrifugation and oven-dried overnight at 120 °C. Their nominal composition is denoted as $Na_2Ti_3O_7$ herein. Sodium-free nanomaterials (denoted as $H_2Ti_3O_7$ herein) were obtained by neutralizing the sodium-based ones in a 0.1 M HCl solution, followed by washing with distilled and deionized water and drying at 120 °C.

To synthesize titania NPs and NWs, approximately 50 mg of either dried sodium-free titanate NT or NW powder was dispersed in 16 mL of distilled water with stirring for 1 h. The solution was then placed in a 23 mL autoclave, which was sealed and heated at 170 °C for 12–36 h. A white precipitate was obtained upon centrifugation. Additional details of the preparation procedure can be found in refs 19 and 20.

**Transmission Electron Microscopy (TEM) Characterization.** Specimens for TEM studies were prepared by depositing a drop of aqueous suspensions of the samples onto a 300 mesh copper grid, coated with a lacey carbon film. Prior to deposition, solutions containing samples were sonicated for 2 min to ensure their adequate dispersion. High-resolution TEM (HRTEM) images were obtained on a JEOL 2010F HRTEM (equipped with an Oxford INCA energy-dispersive spectrometry system) at an accelerating voltage of 200 kV.

TEM images of sodium-free NPs and of NWs are shown in Figure 1; those of sodium-free and -based NTs are shown in Figure 2. TEM revealed that sodium-free NPs are rounded in shape and have an average size of approximately 12 nm. Sodium-free NWs were somewhat larger: a few microns long and approximately 40–500 nm in diameter. Atoms in both the NPs and NWs are seen forming a rather uniform, periodic lattice. In other words, both NPs and NWs (sodium-free) studied here exhibit very good crystallinity. It is disrupted close to their exposed surfaces only.

By contrast, as is observed in Figure 2, sodium-free NTs are tens to hundreds of nanometers long with outer and inner diameters of approximately 7–10 and 3–5 nm, respectively. Their walls are composed of up to three to five atomic layers only, rendering the NTs relatively fragile. Soduim-based NTs are also tens to hundreds of nanometers long but have much thicker walls, making them more stable mechanically. Atomic layers forming the walls of both sodium-free and -based nanotubes run parallel to their long axis. The layers, however, are seen to undulate somewhat, indicating

(7) Fujishima, A.; Honda, K. *Nature* **1972**, *37*, 238.
(8) Dagan, D.; Tomkiewics, M. *J. Phys. Chem.* **1993**, *97*, 12651.
(9) Fukushima, K.; Yamada, I. *J. Appl. Phys.* **1989**, *65*, 619.
(10) Gateshki, M.; Yin, S.; Ren, Y.; Petkov, V. *Chem. Mater.* **2007**, *19*, 2512.
(11) Kasuga, T.; Hiramatsu, A.; Hoson, A.; Sekino, T.; Niihara, K. *Adv. Mater.* **1999**, *11*, 1307.
(12) Du, G. H.; Chen, Q.; Che, R. C.; Yuan, Z. Y.; Peng, L.-M. *Appl. Phys. Lett.* **2001**, *79*, 3702.
(13) Seo, D.-S.; Lee, J.-K.; Kim, H. *J. Cryst. Growth* **2001**, *229*, 428.
(14) Yao, B. D.; Chan, Y. F.; Zhang, X. Y.; Zhang, W. F.; Yang, Z. Y.; Wang, N. *Appl. Phys. Lett.* **2003**, *82*, 281.
(15) Wang, W.; Varghese, O. K.; Paulose, M.; Grimes, C. A. *J. Mater. Res.* **2004**, *19*, 417.
(16) Liu, S. M.; Gan, L. M.; Liu, L. H.; Zhang, W. D.; Zeng, H. C. *Chem. Mater.* **2002**, *14*, 1391.
(17) Wang, Y. Q.; Hu, G. Q.; Duan, X. F.; Sun, H. L.; Xue, Q. K. *Chem. Phys. Lett.* **2002**, *365*, 427.
(18) Sun, X.; Li, Y. *Chem.—Eur. J.* **2003**, *9*, 2229.
(19) Mao, Y.; Wong, S. S. *J. Am. Chem. Soc.* **2006**, *128*, 8217.
(20) Mao, Y.; Kanungo, M.; Hemraj-Benny, T.; Wong, S. S. *J. Phys. Chem. B.* **2006**, *110*, 702.

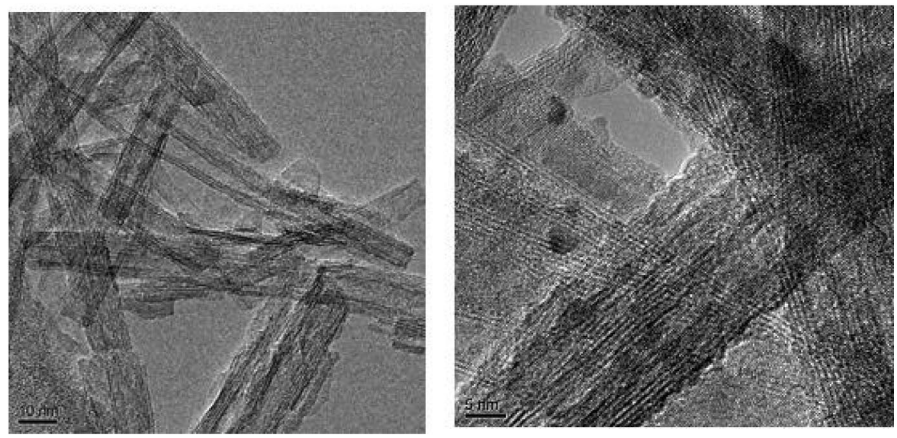

**Figure 2.** TEM images of nanotubes: sodium-free (left) and sodium-based (right).

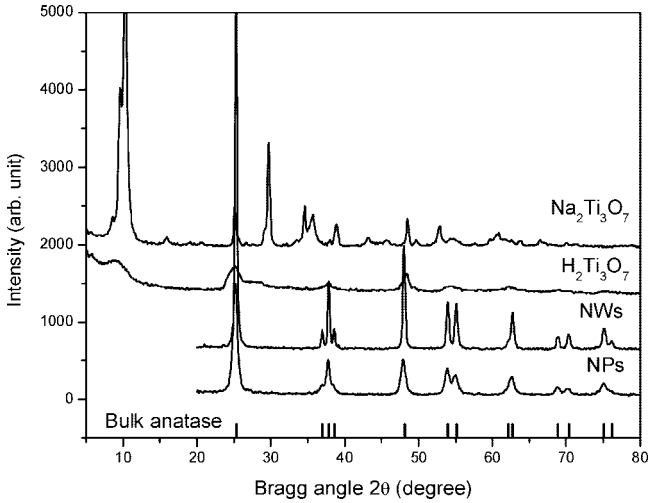


**Figure 3.** In-house XRD patterns of $TiO_2$ NPs, $TiO_2$ NWs, sodium-free and -based titanate nanotubes. The positions of the peaks in the XRD pattern of the anatase polymorph of bulk $TiO_2$ are shown (bars) for comparison.

that the atomic arrangement inside the NTs is not as perfect as that in the NPs and NWs. The interlayer separations in the sodium-free and -based NTs, as revealed by TEM, are ~7.5 and ~9 Å, respectively.

**XRD Experiments.** Nanosized $TiO_2$-type materials were first measured using an in-house source of X-rays (copper anode tube). Experimental data are shown in Figure 3. The XRD patterns for sodium-free NPs and NWs exhibit well-defined Bragg peaks that are also observed in the XRD pattern of anatase (space group $I4_1/amd$; JCPDS No. 21-1272). As a reference, anatase, together with rutile and brookite, is one of the three stable polymorphs of bulk titania. As illustrated in Figure 4, all three are 3D networks of $TiO_6$ octahedra with the network coupling schemes differing slightly among the different polymorphs. Thus, in-house XRD data help to identify the regular lattice fringes in TEM images (Figure 1) of NPs and NWs as atomic planes arising from an anatase-type 3D structure. The Bragg peaks of the anatase structure are sharper in the XRD pattern of NWs as compared with those in the XRD pattern of NPs, which is to be expected because the former are larger (i.e., the anatase structure extends undisturbed over longer distances) in size than the latter (see Figure 1).

The XRD patterns for sodium-free and -based NTs show peaks that do not appear in the corresponding XRD patterns of any of the polymorphs of bulk titania. However, they are similar to the XRD patterns of some layered titanates, such as orthorhombic lepidocrocite ($H_xTi_{2-x/4}\square_{x/4}O_4$; $x \sim 0.7$; $\square$ = vacancy)[21–23] and monoclinic titanate $H_2Ti_3O_7$.[24–28] Thus, in-house XRD enables a rather straightforward determination of the fact that NTs do not exhibit the 3D structure of NPs and NWs. Interestingly, the low-angle peak in the XRD patterns for both sodium-free and -based NTs appears at the same Bragg angle ($2\theta$) of approximately ~10°, indicating that the atomic layers forming the walls of both types of NTs are separated by the same distance of ~9.5 Å. TEM, however, has determined these separations to be somewhat different (7.5 vs 9.5 Å). The origin of this "discrepancy" is discussed below.

A careful inspection of Figure 3 shows that the XRD patterns for NTs, in particular that for sodium-free ones, are composed of peaks that are broader than ones seen in the corresponding XRD patterns for NWs and NPs. Diffraction patterns of sodium-free-type NTs are difficult to analyze by traditional techniques, such as Rietveld analysis, because these methods primarily interpret sharp Bragg peaks that are not present with these nanoscale samples.

The problem was solved by conducting total XRD experiments followed by an atomic PDF data analysis. To place all samples on similar footing, NPs and NWs were subjected to total XRD experiments and PDF analysis as well. The experiments were carried out at the 11-ID-B beamline (Advanced Photon Source, Argonne National Laboratory) using synchrotron radiation possessing an energy of 90.48 keV ($\lambda = 0.1372$ Å). Synchrotron radiation X-rays were employed for two reasons. First, the high flux of synchrotron radiation X-rays allowed the measurement of the quite diffuse XRD pattern of NTs with a very good statistical accuracy over a relatively short data collection time. Second, the high energy of synchrotron radiation X-rays permitted the collection of data over a wide range (1–30 $Å^{-1}$) of scattering vectors **Q**. Both are important[2,29] for the success of the atomic PDF data analysis employed here.

All samples were sealed between Kapton foils, and measurements were performed in transmission geometry. Scattered radiation was

(21) Ma, R.; Bando, Y.; Sasaki, T. *Chem. Phys. Lett.* **2003**, *380*, 577.
(22) Ma, R.; Fukuda, K.; Sasaki, T.; Osada, M.; Bando, Y. *J. Phys. Chem. B* **2005**, 109.
(23) Zhang, S.; Chen, Q.; Peng, L.-M. *Phys. Rev. B* **2005**, *71*, 014104.
(24) Chen, Q.; Zhou, D.; G. H., W.; Peng, L.-M. *Adv. Mater.* **2002**, *17*, 1208.
(25) Chen, Q.; Du, G. H.; Zhang, S.; Peng, L. M. *Acta Crystallogr., Sect. B: Struct. Sci.* **2002**, *58*, 587.
(26) Zhang, S.; Peng, L. M.; Chen, Q.; Du, G. H.; Dawson, G.; Zhou, W. Z. *Phys. Rev. Lett.* **2003**, *91*, 256103.
(27) Xu, X. G.; Ding, X.; Chen, Q.; Peng, L.-M. *Phys. Rev. B* **2007**, *75*, 035423.
(28) Klug, H. P.; Alexander, L. E. In *X-ray diffraction procedures for polycrystalline and amorphous materials*; John Wiley & Sons: New York, 1974.
(29) Petkov, V. *J. Appl. Crystallogr.* **1989**, *22*, 387.

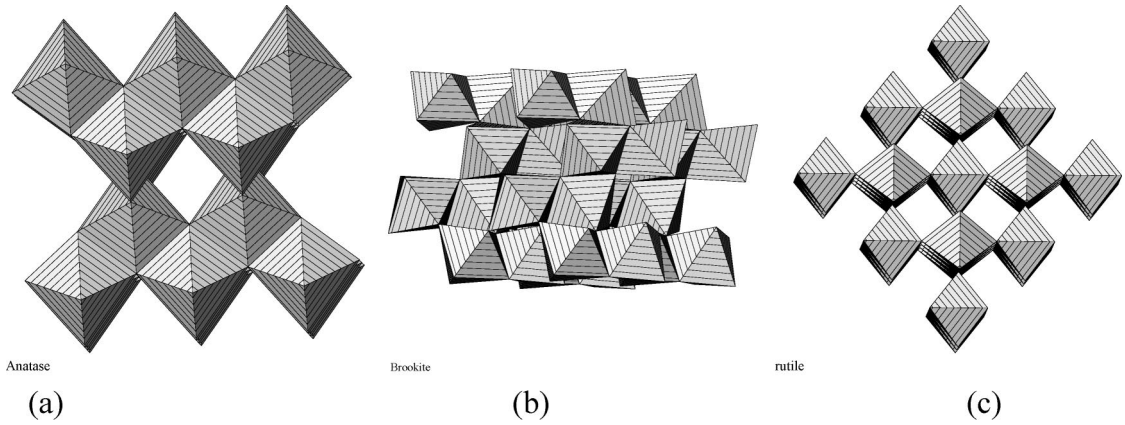


**Figure 4.** Fragments from the (a) anatase, (b) brookite, and (c) rutile polymorphs of bulk titania. All three polymorphs are 3D networks of $TiO_6$ octahedra.

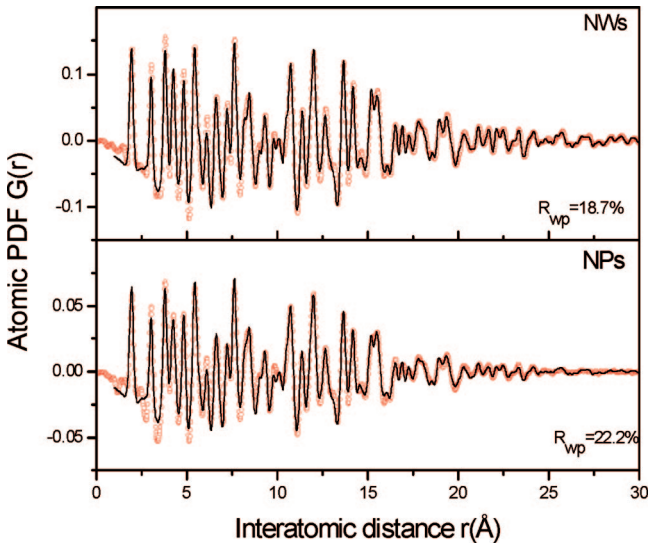


**Figure 5.** Experimental (symbols in red) and model (solid lines in black) PDFs for titania NPs and NWs. The model data are based on the anatase-type structure. The corresponding agreement factors, $R_{wp}$, are reported as well.

collected with a large area detector (General Electric). Up to five images were taken for each of the samples. The corresponding images were combined, subjected to geometrical corrections, reduced to structure factors, and Fourier-transformed to generate atomic PDFs, $G(r) = 4\pi r[\rho(r) - \rho 0]$. Herein, $\rho(r)$ and $\rho_0$ represent the local and average atomic number densities, respectively, and $r$ is the radial distance.[29] All calculations were done with the help of the *RAD* program.[30]

Experimental PDFs for the NPs and NWs are shown in Figure 5, whereas those for the sodium-free and -based NTs are shown in Figures 6 and 7, respectively. Atomic PDFs are composed of several well-defined peaks, each reflecting a frequently occurring interatomic distance in the material studied. In particular, all experimental PDFs possess a first peak positioned at approximately 1.95 Å, which is the Ti–O distance in $TiO_6$ octahedra. The result indicates that atoms in all nanosized materials studied preferably form $TiO_6$ octahedra as they do in bulk $TiO_2$. The question to be answered here is how these octahedra assemble at the nanoscale so that materials of such different morphologies are obtained.

As can be seen in Figure 5, the experimental PDFs for titania NPs and NWs are very well reproduced by a model based on a 3D network of $TiO_6$ tetrahedra, exhibited by the anatase modification of $TiO_2$. The calculations of the model PDFs were performed with the assistance of the *PDFFIT* program.[31] The PDF-based analysis yielded the following structure parameters for the anatase network (S.G. $I4_1/amd$): titania NWs, $a$ = 3.785 Å; $c$ = 9.502 Å, and

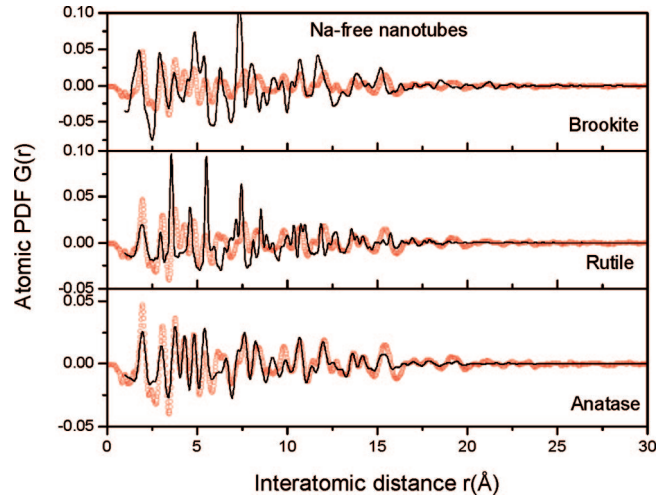


**Figure 6.** Experimental PDF (symbols in red) for sodium-free NTs and model PDFs (lines) computed on the basis of the structure of the three polymorphs of bulk $TiO_2$.

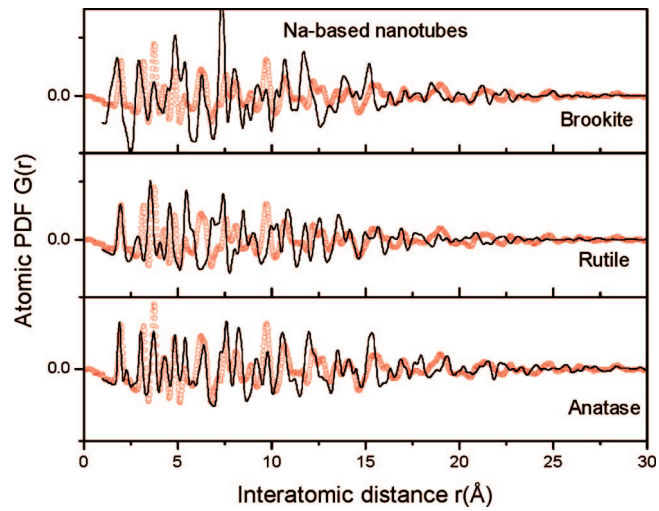


**Figure 7.** Experimental PDF (symbols in red) for sodium-based nanotubes and model PDFs (lines) computed on the basis of the structure of the three polymorphs of bulk $TiO_2$.

(30) Proffen, Th.; Billinge, S. J. L. *J. Appl. Crystallogr.* **1999**, *32*, 572.
(31) Iijima, R. *Nature* **1991**, *354*, 56.

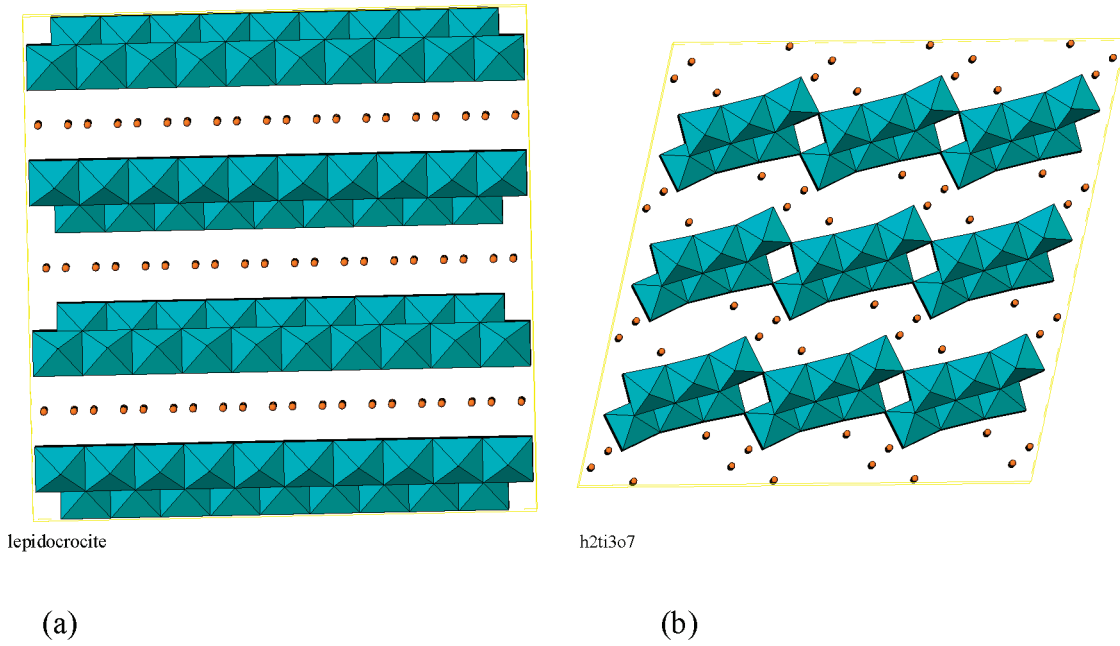


**Figure 8.** Fragments from layered-type structures of (a) lepidocrocite and (b) protonic trititanate $H_2Ti_3O_7$.

Oxygen($z$) = 0.2082; titania NPs, $a$ = 3.782 Å; $c$ = 9.503 Å, and Oxygen($z$) = 0.2086. By comparison, analysis of the PDF data for a standard anatase sample (Sigma) measured on the same instrument yielded $a$ = 3.782 Å; $c$ = 9.503 Å, and Oxygen($z$) = 0.2086. As can be seen in Figures 6 and 7 and from the in-house XRD data analysis, the atomic PDFs of NTs could not be described by a model based on any of the three stable polymorphs of bulk titania. Obviously, contrary to carbon nanotubes[32] and to bulk carbon (i.e., graphite), which are both built from stacks of graphene sheets, flat and rolled, respectively, "$TiO_2$-type" NTs and bulk $TiO_2$, regardless of their very similar chemical composition, are considerably more distinctive from a structural point of view.

## Discussion

To determine the 3D structure of NTs, we, prompted by the results of the preliminary analysis of the PDF data, concentrated on structure models based on $TiO_6$ octahedra. The tests were conducted by computing model PDFs and comparing them with the experimental PDF data. Calculations were performed with the assistance of the *PDFFIT* program.[31] Structure model parameters including lattice constants and atomic positions were adjusted to achieve the best possible agreement between the model and experimental PDFs while keeping the inherent symmetry of the models intact. The limited length of structural coherence in the nanotubes, including the presence of disorder (seen close to the exposed surface of NTs; cf. Figures 1 and 2), was taken into account, as discussed in refs 33 and 34. Initially, sodium-free NTs were approached with a model based on the structure of orthorhombic lepidocrocite $H_xTi_{2-x/4}\square_{x/4}O_4$ ($x \sim 0.7$, $\square$ = vacancy)[21–23] because both materials were found to produce similar XRD patterns. Lepidocrocite may be best described as a stack of flat layers of $TiO_6$ octahedra, as shown in Figure 8a. The model did reproduce most of the basic features of the experimental data (see Figure 9) but failed in several important details, especially at short interatomic distances (see Figure 9). Another flat layer-type model based on orthorhombic $H_2Ti_2O_5 \cdot H_2O$[35] performed somewhat better but was not sufficiently adequate to fit our data either.

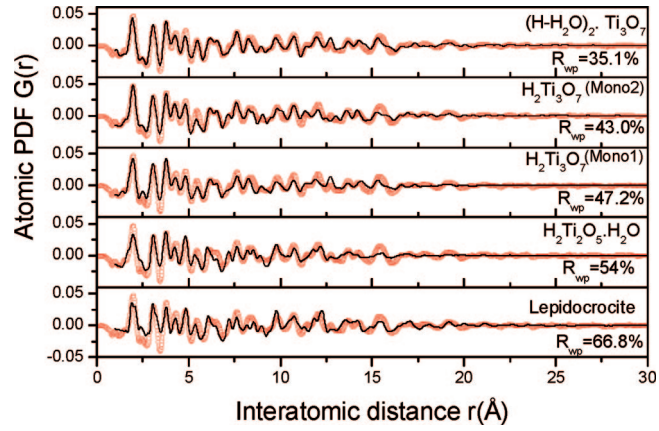


**Figure 9.** Experimental PDF (symbols in red) for sodium-free titania NTs and model PDFs (lines), computed on the basis of several structure types as discussed in the text. The corresponding agreement factors $R_{wp}$ are shown as well.

Acceptable results were, nevertheless, achieved when models featuring corrugated layers of $TiO_6$ octahedra (see Figure 8b) based on monoclinic $H_2Ti_3O_7$ (space group $P2_1/m$) were used. Two such models, referred to as Mono(1) and Mono(2) in Table 1, were attempted. The two differ in the positions of the H atoms between the layers of octahedra.[24] Because $H_2Ti_3O_7$ and $Na_2Ti_3O_7$ are two closely related structures and because sodium-free NTs are obtained by ion exchange, i.e., by replacing interlayer $Na^+$ ions in $Na_2Ti_3O_7$ with $H^+$, the monoclinic $Na_2Ti_3O_7$-type structure model was tried as well. The stoichiometry of sodium-free NTs was

(32) Gateshki, M.; Chen, Q.; Peng, L.-M.; Chupas, P.; Petkov, V. *Z. Kristallogr.* **2007**, submitted for publication.
(33) Gateshki, M.; Hwang, S.-J.; Park, D. H.; Ren, Y.; Petkov, V. *Chem. Mater.* **2004**, *16*, 5153.
(34) Chien-Cheng, T.; Teng, H. *Chem. Mater.* **2006**, *18*, 367.
(35) Suzuki, Y.; Yoshikawa, S. *J. Mater. Res.* **2004**, *19*, 982.

**Table 1. Lattice Parameters of Structure Models of Sodium-Free[a] and -Based Titanate Nanotubes As Obtained by PDF Analysis**

| | | lattice parameters (Å) | |
|---|---|---|---|
| sample | model type | nanotubes | bulk |
| sodium-free NTs | lepidocrocite (orthorhombic) $H_xTi_{2-x/4}x/4O_4 \cdot H_2O$ | $a = 3.811$, $b = 18.676$, $c = 3.0261$ | $a = 3.829$, $b = 17.012$, $c = 2.962$[21] |
| | $H_2Ti_2O_5 \cdot H_2O$ (orthorhombic) | $a = 18.481$, $b = 3.800$, $c = 3.017$ | $a = 18.08$, $b = 3.797$, $c = 2.998$[35] |
| | $H_2Ti_3O_7$ [Mono(1)], $H_2Ti_3O_7$ [Mono(2)] | $a = 8.897$, $b = 3.805$, $c = 10.241$, $\beta = 101.58°$; $a = 8.264$, $b = 3.788$, $c = 9.450$, $\beta = 101.50°$ | $a = 8.998$, $b = 3.764$, $c = 9.545$, $\beta = 102.65°$;[24] $a = 8.771$, $b = 3.733$, $c = 9.759$, $\beta = 101.42°$[24] |
| | $(H–H_2O)_2Ti_3O_7$ | $a = 8.934$, $b = 3.792$, $c = 10.241$, $\beta = 101.26°$ | $a = 8.7403$, $b = 3.8788$, $c = 9.3197$, $\beta = 101.40°$[37] |
| sodium-based NTs | $Na_2Ti_3O_7$ (a) | $a = 8.219$, $b = 3.738$, $c = 9.769$, $\beta = 101.42°$ | $a = 9.133$, $b = 3.806$, $c = 8.566$, $\beta = 101.57°$[38] |
| | $Na_2Ti_3O_7$ (b) | $a = 9.097$, $b = 3.749$, $c = 9.925$, $\beta = 101.58°$ | $a = 8.7403$, $b = 3.8788$, $c = 9.3197$, $\beta = 101.40°$[37] |
| | $Na_2Ti_3O_7$ (b) $r = 1$–10A | $a = 9.026$, $b = 3.738$, $c = 9.908$, $\beta = 101.55°$ | |
| | $Na_2Ti_3O_7$ (b), $r = 10$–30 Å | $a = 9.186$, $b = 3.7502$, $c = 9.947$, $\beta = 101.623°$ | |

[a] Literature data for the corresponding bulk materials are also shown for comparison.

**Table 2. Fractional Coordinates of Atoms/Molecules inside the Unit Cell of Monoclinic $(H–H_2O)_2Ti_3O_7$ (Space Group $P2_1/m$) As Obtained by PDF Analysis**

| atom/molecule | $x$ | $z$ |
|---|---|---|
| $(H–H_2O)$ | 0.5088 | 0.7795 |
| $(H–H_2O)$ | 0.1734 | 0.4761 |
| Ti | 0.0299 | 0.2687 |
| Ti | 0.2362 | 0.6738 |
| Ti | 0.1497 | 0.9873 |
| O1 | 0.2340 | 0.1820 |
| O2 | 0.1850 | 0.4457 |
| O3 | 0.4280 | 0.6797 |
| O4 | 0.2767 | 0.8713 |
| O5 | 0.0300 | 0.7474 |
| O6 | 0.8200 | 0.3458 |
| O7 | 0.0504 | 0.0504 |

[a] All atoms/molecules occupy the position ($\pm x$, 0.25, $z$).

achieved by replacing Na atoms in the model structure with $H^+$ ions and, in a next step, by adding some $H_2O$ molecules. The latter step was undertaken to further improve the $H^+$-based model and to take into account suggestions of several studies[13,19,25–27,36] that layered materials prepared by hydrothermal and ion-exchange methods are very likely to contain water encapsulated between the layers. This model, referred to as $(H–H_2O)_2Ti_3O_7$ in Table 1, was the best fit of all (note the agreement factors $R_{wp}$ reported in Figure 9).

The refined values for the lattice parameters of the model are listed in Table 1. The positions of atoms inside the unit cell are shown in Table 2. Thus, according to the PDF-guided structure search, the walls in the sodium-free "$TiO_2$-type" NTs are composed of corrugated layers of $TiO_6$ octahedra that are approximately 10 Å apart and encapsulate a fair amount of water molecules. TEM studies, on the other hand, suggest an interlayer distance of approximately 7.5 Å. The total XRD/PDF and TEM results apparently disagree but indeed are both correct. That is, sodium-free NTs appear to contain water as obtained and, hence, show a "swelled" (~10 Å) interlayer separation when measured by XRD on samples in their natural environment. By contrast, TEM experiments are carried out in high vacuum and under an intense beam of electrons that bombards and thereby considerably heats the samples studied. Under such experimental conditions,

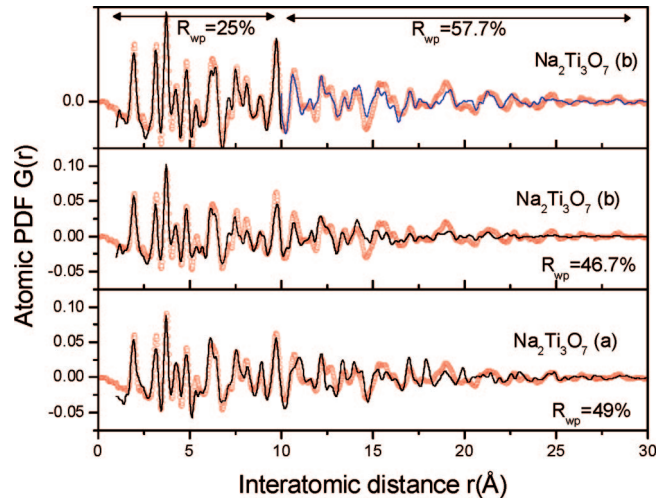


**Figure 10.** Experimental PDF (symbols in red) for sodium-based NTs and model PDFs (lines) computed on the basis of two slightly different monoclinic-type structures discussed in the text. The corresponding agreement factors $R_{wp}$ are shown as well.

**Table 3. Fractional Coordinates of Atoms inside the Unit Cell of Monoclinic $Na_2Ti_3O_7$ (Space Group $P2_1/m$), As Obtained by PDF Analysis**

| atom | $x$ | $z$ |
|---|---|---|
| Na | 0.7920 | 0.6278 |
| Na | 0.2770 | 0.5418 |
| Ti | 0.9525 | 0.1146 |
| Ti | 0.6621 | 0.2327 |
| Ti | 0.2832 | 0.0681 |
| O1 | 0.1747 | 0.1583 |
| O2 | 0.5299 | 0.2364 |
| O3 | 0.6569 | 0.4553 |
| O4 | 0.8821 | 0.2586 |
| O5 | 0.7568 | 0.0743 |
| O6 | 0.3708 | 0.8229 |
| O7 | 0.0855 | 0.9661 |

[a] All atoms occupy the position ($\pm x$, 0.25, $z$).

water is known to evaporate. As a result, the initially "hydrated" NTs lose water and appear with an interlayer separation "shrunk" to approximately 7.5 Å.

Logically, sodium-based NTs were approached with models based on layered sodium titanates[24,37,38] and it was found that a monoclinic $Na_2Ti_3O_7$-type model reproduces the experimental data rather well. In fact, from the two slightly

(36) Andersson, S.; Wadsley, A. D. *Acta Crystallogr.* **1961**, *14*, 1245.

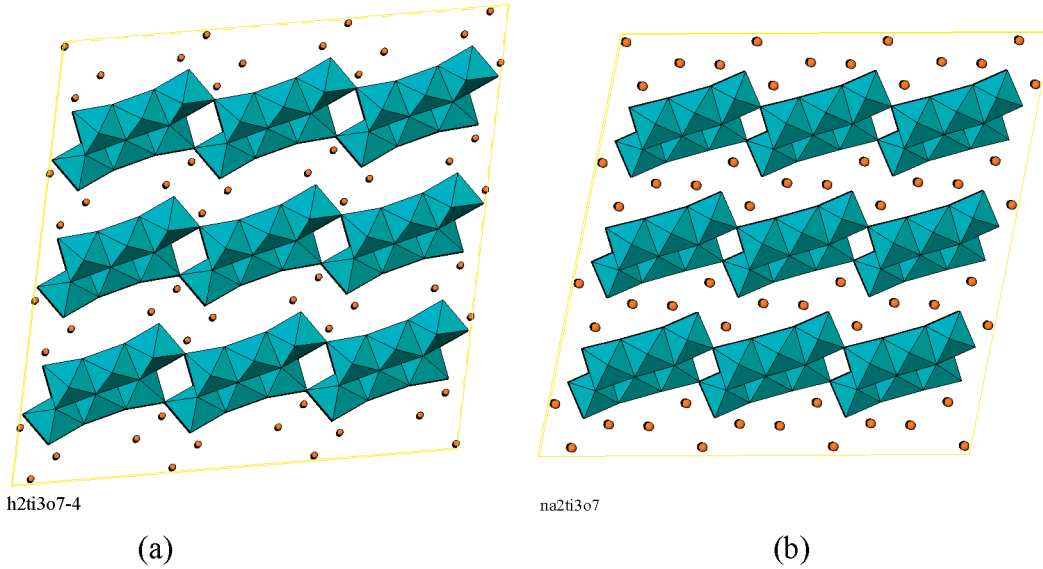


**Figure 11.** Fragments of the walls of sodium-free (left) and sodium-based (right) titanate nanotubes as determined from the present total XRD/PD studies. The walls are built from corrugated layers of $TiO_6$ octahedra and encapsulate "Water & Protons" and Na atoms, respectively (shown as small circles).

different $Na_2Ti_3O_7$-type structures reported in the literature, that of Andersson and Wadsley[36] (marked as "b" in Figure 10) outperformed the one of Yakubovich and Kireev[37] (marked as "a" in Figure 10).

Structural parameters of model b as refined against the experimental PDF data are summarized in Tables 1 and 3. Interestingly, model b was found to perform much better at shorter (<10 Å) as opposed to longer (>10 Å) interatomic distances (see Figure 10). Such behavior has been previously observed with other nanosized oxide materials.[10,34,39] Herein, it suggests that the otherwise perfect layers of octahedra forming the walls of sodium-based NTs are not lined up in perfect registry, leading to a weakening of the layer–layer correlations that start appearing at distances longer than ~10 Å. Such a conclusion would be difficult to arrive at, solely on the basis of TEM observations alone.

In summary, total XRD/PDF studies can yield the 3D structure of nanosized materials, even with the complex morphology of nanotubes, in terms of the usual "crystallographic-type" parameters (see Tables 1–3). This compact structural representation allows for a convenient computation, understanding, and prediction of nanomaterials' properties. Dense-filled nanosized materials such as titania NPs and NWs were found to adopt an anatase-type structure that is a 3D network of $TiO_6$ octahedra. In this respect, they may be viewed as nanosized analogues of bulk $TiO_2$. By contrast, hollow nanosized materials such as "$TiO_2$-type" NTs possess a layered-type structure. The layers are built from $TiO_6$ octahedra and exhibit zigzag "steps", as shown in Figure 11. This structural motif is flexible enough to afford a scroll-type morphology, as shown in our previous[33] work as well as in other[24–26] studies. In this respect "$TiO_2$-type" NTs may not be viewed as nanosized analogues of bulk $TiO_2$, in contrast to earlier suggestions.[40] Other oxide NTs such as "$V_2O_5$"-type ones are found to show a similar behavior.[3]

## Conclusions

The total XRD coupled with an atomic PDF data analysis may reveal the 3D structure of nanosized materials of various morphologies. In particular, we find that the chemical composition (i.e., Ti and O in a ratio close to 1:2) and the type of atomic bonding (i.e., ionic) between the chemical species involved predetermine the basic structural building blocks/units (i.e., $TiO_6$ octahedra) in nanosized "$TiO_2$-type" materials. Morphology, however, may favor a particular way in which these building units/bricks are arranged in space. With nanosized but dense-filled "$TiO_2$-type" materials, such as NPs and NWs, the arrangement is a 3D network of octahedra, as it is in bulk $TiO_2$. With nanosized but hollow "$TiO_2$-type" materials, such as nanotubes, a scroll of corrugated layers of $TiO_6$ octahedra is a more likely crystallographic manifestation. Nanosized materials continue to come in even more complex morphologies (e.g., tetrapods,[41] "blackberries", etc.). All of these architectures may and should be subjected to a precise 3D structure determination using the approach reported herein.

**Acknowledgment.** The work was supported by CMU through Grant REF C602281. Use of the Advanced Photon Source was supported by the U.S. Department of Energy, Office of Science, Office of Basic Energy Sciences, under Contract DE-AC02-06CH11357. Research at Brookhaven National Laboratory was supported in part by the U.S. Department of Energy Office of Basic Energy Sciences under Contract DE-AC02-98CH10886 for personnel support. S.S.W. acknowledges the Alfred P. Sloan Foundation (2006–2008) for support of this research. We also thank Professor J. Huang and S. Chen at Boston College for their help with the HRTEM images. The overall assistance of Hongjun Zhou (SUNY at Stony Brook) is also appreciated.

CM7019069

(37) Yakubovich, O. V.; Kireev, V. V. *Kristallografiya* **2003**, *48*, 29.
(38) Gateshki, M.; Petkov, V.; Williams, G.; Pradhan, S. K.; Ren, Y. *Phys. Rev. B* **2005**, *71*, 224107.
(39) Kasuga, T.; Hiramatsu, M.; Hoson, A.; Sekino, T.; Niihara, K. *Langmuir* **1998**, *14*, 3160.
(40) Cozzoli, P.; et al. *Nano Lett.* **2006**, *6*, 1966.
(41) Liu, T.; Diemann, E.; Li, H.; Dress, W. M.; Muller, A. *Nature* **2003**, *426*, 59.